American Journal of Engineering and Applied Sciences

Research Article

Hybrid Adaptive Filters for Dynamic Mass Measurement of Moving Objects on Flexible Platforms

Sergio Bimbi Junior, Flavio Celso Trigo and Agenor de Toledo Fleury

Department of Mechanical Engineering Control and Automation Engineering, University of Sao Paulo (USP), Sao Paulo, Brazil

Article history
Received: 13-11-2025
Revised: 28-01-2026
Accepted: 23-03-2026

Corresponding Author:
Sergio Bimbi Junior
Department of Mechanical Engineering Control and Automation Engineering, University of Sao Paulo (USP), Sao Paulo, Brazil
Email: bimbi@bol.com.br

Abstract: Dynamic mass measurement of moving objects on flexible platforms remains a significant challenge due to mechanical vibrations, structural flexibility, and the inherently low Signal-to-Noise Ratio (SNR) of strain gauge sensors. Traditional analog filtering approaches, such as Tow–Thomas active filters, exhibit limitations since gain stages propagate and may even amplify intrinsic noise, compromising metrological accuracy. This work proposes a hybrid adaptive filtering methodology that integrates a passive input stage, a four-Degree-Of-Freedom (4-DOF) dynamic platform model, and a digitally implemented adaptive Tow–Thomas IIR filter with iterative SNR-based prediction. The passive stage operates as an initial low-pass filter, attenuating high-frequency electromagnetic interference (≈ 724 kHz) and ensuring proper conditioning of the signal for subsequent A/D conversion. The 4-DOF model describes the coupled effects of translational and rotational dynamics of the platform, enabling the use of the Random Decrement technique for modal frequency identification. Finally, the adaptive digital Tow–Thomas filter iteratively updates its coefficients until the specified SNR is achieved, guaranteeing unitary gain and preventing spectral distortions. Simulation results and industrial checkweigher measurement datasets demonstrate that the proposed structure enhances system robustness and improves noise rejection while preserving accuracy in the dynamic quantification of moving masses.

Keywords: Cybersecurity, IEC 61850, SEP, N-NE-SE Interconnection, Goose Adaptive Filters, Dynamic Mass Measurement, Hybrid Analog–Digital Systems, Load Cells, Random Decrement, Tow-Thomas IIR

Introduction

Dynamic mass measurement of moving objects on flexible platforms is an essential requirement in industrial applications, such as checkweigher systems, and in transportation, such as Weigh-in-Motion (WIM). Despite technological progress, the accuracy of these measurements still faces challenges associated with the low Signal-to-Noise Ratio (SNR) of strain-gauge-based sensors, as well as structural vibrations, mechanical flexibility, and electromagnetic interference. These factors compromise metrological accuracy, particularly under high-speed conditions and in noisy environments Halimic and Balachandran (2002); Chen et al. (2019); Deng et al. (2018).

Several approaches have been proposed to mitigate such limitations, including digital filters based on polynomial window modifications Junior et al. (2018), Kalman filters for adaptive noise suppression Halimic and Balachandran (2002); Sun and Deng (2005); Harb (2013), and analog adaptive compensation techniques Jafaripanah et al. (2005). However, each solution has specific constraints: Analog methods, such as the Tow Thomas active filter, may propagate and even amplify noise due to their gain stages; traditional digital filters, such as fixed Finite-Impulse-Response (FIR) and Infinite-Impulse-Response (IIR) structures, lack flexibility to adapt to dynamic operating conditions. Furthermore, in flexible platforms, more realistic models are required to capture the coupled effects of translation, rotation, and support vibrations, since oversimplified models often lead to significant errors in mass estimation Chen et al. (2019); Deng et al.

(2018).

In this work, we propose a hybrid methodology that integrates three key elements:

(i) A passive input filter for initial attenuation of high-frequency interference (≈ 724 kHz)
(ii) A four-degree-of-freedom (4-DOF) dynamic platform model representing coupled effects and enabling modal analysis via Random Decrement Chen et al. (2019); Deng et al. (2018)
(iii) An adaptive digital Tow Thomas Infinite-Impulse-Response (IIR) filter, discretized using the bilinear transform and iteratively adjusted until the specified Signal-to-Noise Ratio (SNR) is achieved

This integration aims to overcome the limitations of conventional methods, providing a robust, scalable, and metrologically consistent solution for the dynamic quantification of moving masses.

The main objective of this work is to design, implement, and evaluate a hybrid adaptive filtering architecture capable of achieving metrological accuracy in dynamic mass measurement under structural flexibility, low Signal-to-Noise Ratio (SNR), and vibrational disturbances. The method aims to ensure unity DC gain, accurate force reconstruction, and robust convergence through an iterative SNR-based adaptation strategy integrated with a 4-DOF platform model.

Main Contributions The main contributions of this work can be summarized as follows:

- Hybrid measurement-chain architecture: A unified framework combining a passive analog RC anti-interference stage, a physically motivated 4-DOF flexible-platform model, and a digital adaptive Tow Thomas IIR biquad implemented on the DSP
- SNR-driven iterative coefficient recalibration: Unlike classical error-driven adaptive filters (e.g., LMS/NLMS), the proposed approach employs an iterative prediction loop that updates the cutoff frequency and redesigns the biquad coefficients until a target SNR is achieved
- Metrological constraint enforcement: The adaptation explicitly guarantees unity DC gain and imposes bounded in-band magnitude response (in dB), preventing artificial spectral distortion and steady-state bias in mass estimation
- Quantitative evaluation under vibration and low-SNR conditions: The method is assessed using SNR improvement, RMSE, and stabilization time under composite signals that include trapezoidal loading, injected noise, and multi-harmonic vibration disturbances

Related Work

Mass quantification in dynamic systems has been a recurring research topic due to structural perturbations, vibrations, and the low Signal-to-Noise Ratio (SNR) present in signals obtained from load cells. These conditions impose significant restrictions on metrological accuracy, especially in platforms subjected to structural flexibility and external excitations Chen et al. (2019); Deng et al. (2018); Ikeda et al. (1992). Recent research in Weigh-in-Motion (WIM) systems further highlights that field deployment introduces additional uncertainties, including vehicle bridge interaction variability, temperature effects, and sensor mounting conditions, which may significantly affect identification accuracy Shi et al. (2025); Chen et al. (2025).

Classical digital filtering solutions, such as Finite-Impulse-Response (FIR) filters, have been applied to suppress noise in low-amplitude signals, with advances based on polynomial window modifications that enlarge the convergence region and improve stability Junior et al. (2018). Although FIR filters are inherently stable and can preserve linear phase, they often require high orders to achieve steep attenuation, increasing computational cost and convergence time in highly dynamic weighing scenarios. Infinite-Impulse-Response (IIR) filters provide greater computational efficiency but are often constrained by stability margins and the need for fine tuning of their coefficients Oppenheim and Schafer (1999); Proakis and Manolakis (2006). In industrial checkweigher applications, periodic disturbances have been addressed using digital multiple IIR notch filtering structures, showing improved rejection of deterministic vibration-induced noise in experimental platforms Sun et al. (2020).

The introduction of adaptive filtering techniques represented a major step forward compared with fixed-parameter methods. Algorithms such as Least Mean Squares (LMS), Normalized LMS (NLMS), and Recursive Least Squares (RLS) enable real-time adaptation to signal variations and noise conditions, enhancing robustness in dynamic mass quantification systems Haykin (2013). Kalman filters have also been successfully employed, allowing uncertainties to be treated as stochastic processes and improving reliability of estimates in environments with strong vibrational components Halimic and Balachandran (2002); Sun and Deng (2005); Harb (2013). More recently, hybrid strategies combining FIR preprocessing with Kalman filtering have been proposed 2 Sergio Bimbi Junior, Fl ´ avio Celso Trigo, Agenor de Toledo

Fleury/ American Journal of Engineering and Applied Sciences 2018, 14 (3): Page Numbers ´ DOI: To increase measurement accuracy in dynamic weighing processes, reinforcing the relevance of hybrid filtering architectures for industrial prediction algorithms (Zengin and Akdemir, 2025).

In the analog domain, Jafaripanah et al. (2005) demonstrated the use of active adaptive filters for dynamic sensor compensation but highlighted critical limitations related to propagation and amplification of noise across gain stages. These drawbacks reinforced the shift toward digital implementations, where discretization and algorithmic control mitigate noise amplification while improving stability. Additionally, system-level modeling and identification have gained importance in the last decade, since accurate mechanical representations are required to correctly separate structural dynamics from the true weight component.

In this context, recent advances in vibration characterization and modal identification under environmental excitation continue to rely on the Random Decrement Technique (RDT), with improvements that combine RDT with Stochastic Subspace Identification (SSI) in order to reduce mode omission and false-mode detection Wu et al. (2025). Such methods provide a basis for obtaining more reliable modal parameters and quantifying uncertainty bounds in identified modes, which is essential for robust modeling of flexible measurement platforms Xu et al. (2025).

Therefore, although FIR, IIR, Kalman, and analog compensation approaches have made significant contributions to the field, gaps remain regarding spectral fidelity preservation and explicit gain control in decibels (dB), particularly when the measurement platform dynamics exhibit coupled translational and rotational modes. In this context, the present work proposes an approach that combines iterative prediction based on the Signal-to-Noise Ratio (SNR) with explicit metrological constraints, ensuring unitary gain and preventing artificial distortions or attenuations in dynamic mass quantification.

System Modeling

The measurement chain comprises:

(i) A strain-gauge Wheatstone bridge transducer
(ii) A passive first-order RC input filter
(iii) A 24-bit Analog-to-Digital Converter (ADC) sampling at 600 Hz followed by a Digital Signal Processor (DSP), where the adaptive Tow–Thomas Infinite-Impulse-Response (IIR) biquad is implemented
(iv) The measurement system proper, modeled as a four-Degree-Of-Freedom (4-DOF) flexible platform that generates the dynamic force acting on the transducer. The adaptive filter operates on the digitized transducer signal and reacts to the dynamics imposed by the 4-DOF model while enforcing metrological constraints (unity DC gain and bounded magnitude in decibels) Oppenheim and Schafer (1999); Meirovitch (2001); Rao (2011); Helfrick and Cooper (1990)

For small strains, a Wheatstone bridge excited with Vexc yields a differential output approximately linear with the strain $\varepsilon(t)$ Helfrick and Cooper (1990):

Strain-Gauge Transducer and Bridge Relation

$$\frac{\Delta R}{R} \approx G\varepsilon(t), V_S(t) \approx \frac{V_{exc}}{4}\left(\frac{\Delta R}{R}\right) = \frac{GV_{exc}}{4}\varepsilon(t) \tag{1}$$

Where G is the gauge factor. Assuming a linear relationship $\varepsilon(t) = \alpha F(t)$ between the equivalent force $F(t)$ at the sensor and the strain, one obtains:

$$v_s(t) = kF(t), \quad \kappa \equiv \frac{GV_{exc}}{4\alpha}\left[V/N\right] \tag{2}$$

Where κ is the transduction gain. The force $F(t)$ is provided by the 4-DOF platform model.

Passive RC Input Filter and Anti-Interference Stage

The transducer output is applied to a first-order RC low-pass filter whose transfer function is:

$$H_{RC}(s)=\frac{1}{1+sRC} \tag{3}$$

Its cutoff frequency is given by:

$$f_c=\frac{1}{2\pi RC} \tag{4}$$

For R = 220 Ω and C = 1 nF, one Obtains $f_c \approx 7.24\frac{dy}{dx}\times 10^5\, Hz$.

This stage attenuates high-frequency electromagnetic interference, while leaving the band of interest (from a few hertz to a few hundred hertz) essentially unaltered.

When a discrete-time representation is required (e.g., for simulation alignment), the bilinear transform maps s to z Oppenheim and Schafer (1999):

$$s \leftarrow \frac{2}{T_s}\frac{1-z^{-1}}{1+^{z-1}}, T_S=\frac{1}{600}s \tag{5}$$

This substitution yields a discrete-time first-order $H_{RC}(z)$ consistent with (3) and (4).

Sampling and quantization 24-bit Analog-to-Digital Converter (ADC) at 600 Hz.

Let the Analog-to-Digital Converter (ADC) full-scale reference be Vref = 5 V and resolution N = 24. The quantization step is:

$$q=\frac{V_{ref}}{2^N}=\frac{5}{2^{24}}V \approx 2.98\times 10^{-7}V \tag{6}$$

The quantization-noise variance is given by:

$$\sigma_q^2=\frac{q^2}{12}$$

The discrete-time sequence at the DSP input is:

$$\chi[n]=Q\{(h_{RC} * V_s)(nT_s)+n_a(nT_S)\} \tag{7}$$

Where $Q\{\cdot\}$ denotes quantization, h_{RC} is the impulse response of $H_{RC}(s)$ defined in (3), and $n_a(t)$ aggregates residual analog noises (thermal and EMI remnants), all filtered by H_{RC}.

Four-DOF Flexible Platform and Equivalent Transducer Force

The measurement system is a 4-DOF platform with generalized coordinates: Vertical translation $z(t)$ (center of mass), rotation $\theta(t)$ about the center, and vertical motions of the left/right supports $z_1(t)$, $z_2(t)$. With platform mass m, inertia I, support masses m_1, m_2, stiffnesses k_1, k_2, dampings c_1, c_2, and half-spacing d/2, the equations of motion (Newton's second law) are Meirovitch (2001); Onate et al. ˜ (1993).

Platform Translation:

$$m\ddot{z}(t)=-k_1\left(z-z_1+\frac{d}{2}\theta\right)-k_2\left(z-z_2-\frac{d}{2}\theta\right)-c_1\left(z-z1+\frac{d}{2}\theta\right)-c_2\left(z-z_2-\frac{d}{2}\theta\right)+u(t) \tag{8}$$

Platform Rotation:

$$1\ddot{\theta}(t)=-k_1\left(z-z_1+\frac{d}{2}\theta\right)\left(\frac{d}{2}\right)+k_2\left(z-z_2-\frac{d}{2}\theta\right)\left(\frac{d}{2}\right)-c_1\left(z-z_1+\frac{d}{2}\theta\right)\left(\frac{d}{2}\right)+c_2\left(z-z_2-\frac{d}{2}\theta\right)\left(\frac{d}{2}\right) \tag{9}$$

Left support:

$$m_1\ddot{z}_1 = k_1\left(z - z_1 + \frac{d}{2}\theta\right) + c_1\left(z - z_1 + \frac{d}{2}\theta\right) \tag{10}$$

Right Support:

$$m_2\ddot{z}_2(t) = \left(z - z_2 - \frac{d}{2}\theta\right) + c_2\left(z - z_2 - \frac{d}{2}\theta\right) \tag{11}$$

Define the state vector as:

$$\chi(t) = \begin{pmatrix} z(t) \\ \theta(t) \\ z_1(t) \\ Z_2(t) \\ \dot{z}(t) \\ \dot{\theta}(t) \\ \dot{z}_1(t) \\ \dot{z}_2(t) \end{pmatrix} \tag{12}$$

Then the Compact State-Space Form is:

$$\dot{\chi}(t) = A\chi(t) + Bu(t) \tag{13}$$

With *A* and *B* derived from m, m_1, m_2, *I*, k_i c_i, and *d* Meirovitch (2001); Onate et al. (1993).

The equivalent force at the transducer exciting the bridge via (2) is the sum of elastic and viscous contributions at the supports: Figure 1 illustrates the four-Degree-Of-Freedom (4-DOF) platform geometry and the corresponding force diagram, supporting the dynamic model:

$$F(t) = k_1\left(z - z_1 + \frac{d}{2}\theta\right) + k_2\left(z - z_2 - \frac{d}{2}\theta\right) - c_1\left(z - z_1 + \frac{d}{2}\theta\right) + c_2\left(z - z_2 - \frac{d}{2}\theta\right) \tag{14}$$

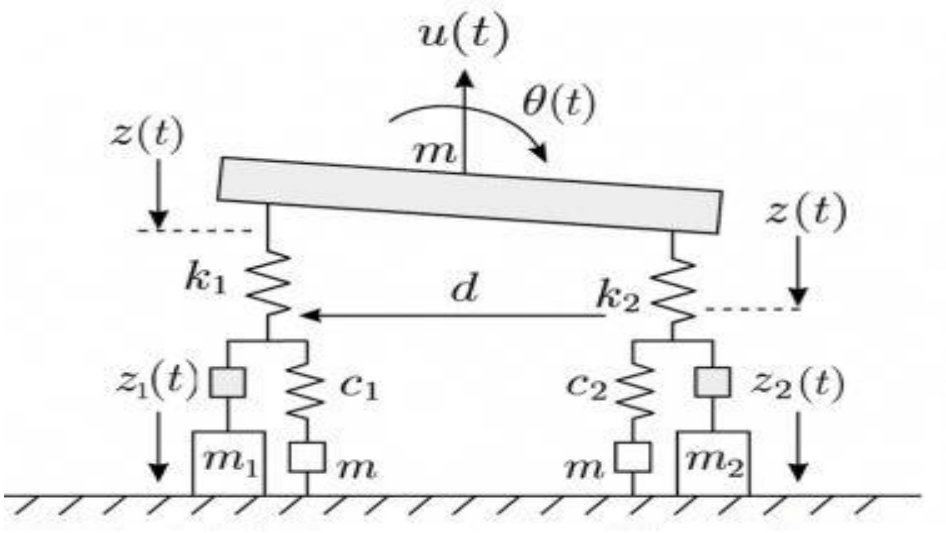

Fig. 1: 4-DOF geometry and force diagram

Complete Measurement Equation and DSP Input

Combining (1), (3) (4), and (14), the analog signal entering the Analog-to-Digital Converter (ADC) is:

$$v_f(t) = (h_{RC} * \kappa F)(t) + n_a(t) \tag{15}$$

With $n_a(t)$ denoting residual analog noise. The sampled/quantized sequence feeding the adaptive filter is given by (7).

Metrological Constraints for the Adaptive Tow Thomas Biquad

In the DSP, the adaptive Tow Thomas Infinite-Impulse Response (IIR) biquad $H_{TT}(z;\theta_k)$ processes $x[n]$ and returns $y[n]$. To guarantee metrological fidelity, two constraints are enforced throughout adaptation:

Unity DC Gain (0 dB):

$$G_0 \triangleq \frac{b_0+b_1+b_2}{1+a_1+a_2} = 1 \tag{16}$$

In-band magnitude bound (in decibels), preventing artificial spectral distortions or attenuations within the 4 Sergio Bimbi Junior, Fl ´ avio Celso Trigo, Agenor de Toledo Fleury/ American Journal of Engineering and Applied Sciences 2018, 14 (3): Page Numbers ´ DOI: measurement band. This constraint is explicitly enforced through the magnitude bound of Eq. (17), which prevents artificial spectral distortions within the measurement band:

$$20\log_{10}\left|H_{TT}(e^{j\omega};\theta_k)\right| \le G_{\max}, \quad \omega \in \Omega_{meas} \tag{17}$$

Where (b_i,a_i) are the normalized bilinear-discretized Tow–Thomas coefficients Proakis and Manolakis (2006), and Ωmeas denotes the measurement band of interest. The update law and the Signal-to-Noise-Ratio (SNR) based performance criterion are detailed in Adaptive Digital Filtering. The dynamic behavior of the Tow-Thomas Biquad during adaptation is shown in Figure 2, which presents the time response for different parameter updates.

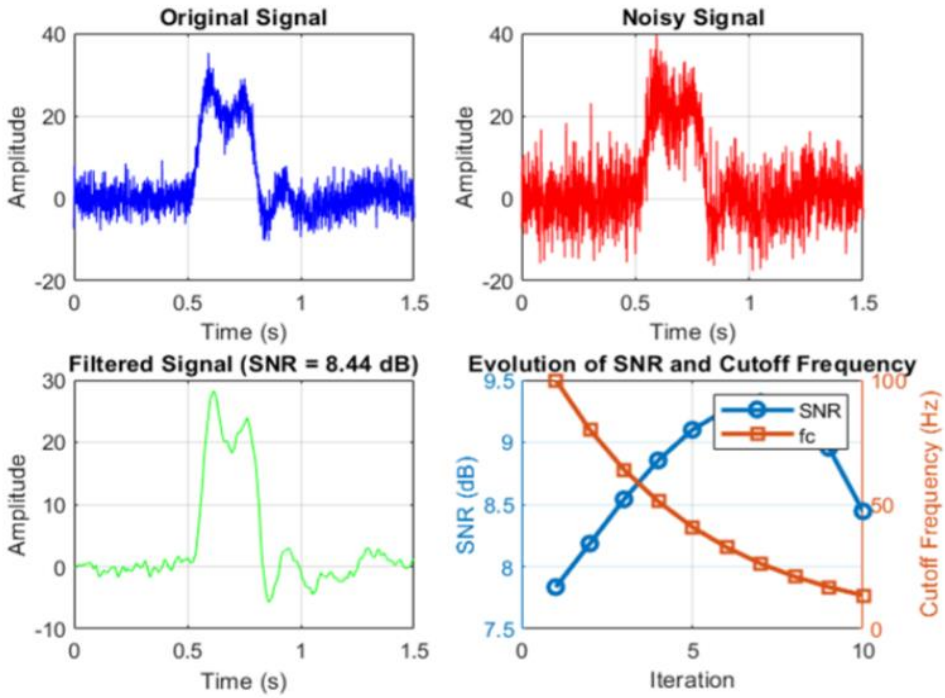

Fig. 2: Response of the Adaptive Tow–Thomas Biquad Filter

Figure 3 presents the Bode magnitude and phase responses of the adaptive Tow-Thomas filter, highlighting the controlled adjustment of the cutoff frequency across iterations.

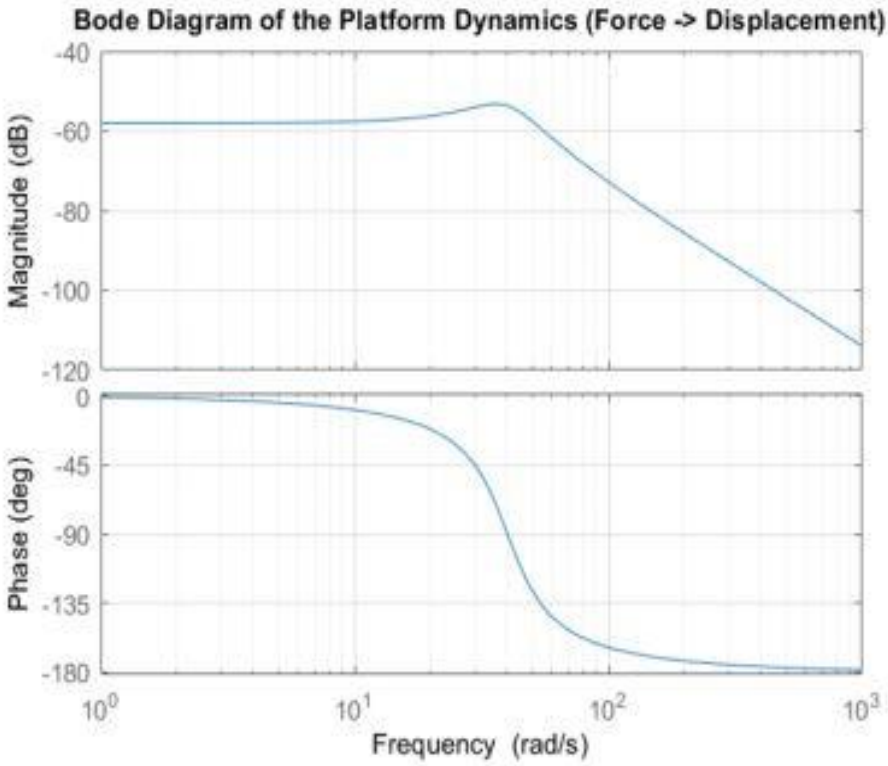

Fig. 3: Bode diagram of the Adaptive Tow–Thomas Biquad Filter

Adaptive Digital Filtering

Tow-Thomas Infinite-Impulse-Response (IIR) Transfer Function

The adaptive filter is based on the Tow–Thomas biquad, whose analog low-pass transfer function is defined as Jafaripanah et al. (2005); Proakis and Manolakis (2006):

$$H_{TT}(s) = \frac{\omega_0^2}{s^2 + 2\xi\ \omega_0 s + \omega_0^2} \tag{18}$$

where $\omega_0 = 2\pi\ f_c$ and ζ is the damping ratio. The bilinear discretization and coefficient normalization steps were detailed in Section 3. Unlike its analog counterpart, the digital implementation avoids noise amplification caused by active stages Jafaripanah et al. (2005) while preserving the efficiency of Infinite-Impulse-Response (IIR) filters Proakis and Manolakis (2006); Haykin (2013).

Iterative Signal-to-Noise Ratio (SNR)-Based Prediction (Coefficient Recalibration)

Pediction (Coefficient Recalibration) The proposed filter introduces an iterative recalibration loop guided by the Signal-to-Noise Ratio (SNR). At iteration k, the output is expressed as:

$$y_k[n] = H_{TT}(z;\theta_k)\chi[n] \tag{19}$$

Where $\theta_k = \{b_0, b_1, b_2, a_1, a_2\}_k$ denotes the coefficients at iteration *k*. The Signal-to-Noise Ratio (SNR) at iteration *k* is computed as Halimic and Balachandran (2002):

$$SNR_k = 10\log_{10}\left(\frac{\sum_n x[n]^2}{\sum(x[n]\text{-}yk[n])^2}\right) \tag{20}$$

If $SNR_k < SNR_{target}$, the cutoff frequency is updated according to:

$$f_{c,k+1} = \alpha_{fc,k}, \quad 0 < \alpha < 1 \tag{21}$$

And new coefficients are designed. The loop terminates when $SNR_k \geq SNR_{target}$ or when a maximum number of iterations is reached.

This predictive mechanism differs from error-driven algorithms such as LMS Oppenheim and Schafer (1999), since it enforces both metrological catestraints (unity DC gain, bounded gain in dB) and SNR convergence. Figure 4 shows the convergence behavior of the adaptive Tow–Thomas biquad filter, illustrating the evolution of the Signal-to-Noise Ratio (SNR) and the corresponding cutoff frequency across iterations.

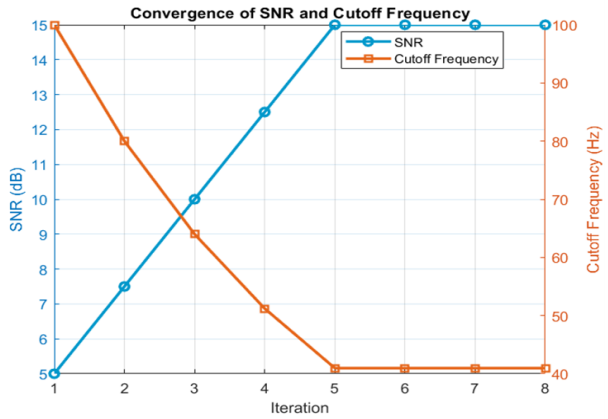

Fig. 4: Convergence of the adaptive Tow-Thomas biquadfilter showing the evolution of the Signal-to-Noise Ratio (SNR) (left axis) and cutoff frequency (right axis) across iterations

Comparison with Finite-Impulse-Response (FIR), Infinite-Impulse-Response (IIR), Kalman and Adaptive Tow-Thomas Biquad Filter

A comparative overview of Finite-Impulse-Response (FIR), Infinite-Impulse-Response (IIR), Kalman, and the proposed adaptive Tow-Thomas filter is presented in Table 1, highlighting advantages, limitations, and typical application scenarios.

Table 1: Comparative summary of Finite-Impulse-Response (FIR), Infinite-Impulse-Response (IIR), Kalman, andadaptive Tow–Thomas biquad filter

Method	Advantages	Limitations	Application Context	Ref.
FIR	Stable, linear phase, flexible design	High order, high computational cost	Usedin checkweighers and situations requiring strict phase linearity	Junior et al. (2018); Haykin (2013)
IIR (fixed)	Low order, efficient implementation	Sensitive to quantization, not adaptive	General-purpose lowpass filtering with compact structure	Proakis and Manolakis (2006); Haykin (2013)
Kalman	Optimal estimation, handles stochastic noise	Requires accurate covariance and system models	Dynamic mass quantification, weigh-in- motion, sensor fusion	Halimic and Balachandran (2002); Ikeda et al. (1992); Sun and Deng (2005); Harb (2013)
Adaptive Tow Thomas	Efficient, SNRadaptive, unity DC gain	Requires iterative design loop, cutoff frequency tuning	Proposed method for dynamic mass measurement with metrological constraints	Jafaripanah et al. (2005); Proakis and Manolakis (2006); Rao (2011); Onate et al. (1993)

DOI: 10.3844/ajeassp.2026.57.72

Materials and Methods

Bench Test Description

The weighing system was reproduced in a MATLAB/Simulink simulation environment, faithfully modeling the physical bench test. The simulated setup emulates:

- Flexible conveyor platform, modeled as a four-Degree-Of-Freedom (4-DOF) structure
- Strain-gauge load cell in Wheatstone-bridge configuration, with excitation voltage Vexc = 5
- Passive RC input filter, designed as a first-order low-pass with cutoff fc ≈ 7.24 × 105 Hz, included in the signal chain to attenuate high-frequency disturbances
- 24-bit Analog-to-Digital Converter (ADC), sampling at 600 Hz, with reference Vref = 5 V, yielding the quantization step q ≈ 2.98×10−7 V
- DSP implementation, simulated by MATLAB routines written in C-style code, executing the adaptive Tow–Thomas biquad filter with iterative Signal-to-Noise Ratio (SNR) recalibration

This simulation bench allows controlled experiments in which structural dynamics, disturbances, and filtering strategies can be evaluated with precision before hardware deployment.

Test Signals

The test signals were generated directly in MATLAB to replicate the operating conditions of a conveyor-based weighing system. The main simulated profiles were:

- Reference mass signals: Modeled as trapezoidal force pulses u(t) corresponding to calibrated weights (0.5–5 kg) moving at constant velocity (1 m/s) across the platform
- Injected Gaussian noise: White noise added digitally at amplitudes between 0.1 and 0.5 V, simulating electromagnetic interference and sensor electronic noise Helfrick and Cooper (1990)
- Vibrational excitation: Multi-harmonic base motion applied to the supports, combining 50 Hz, 120 Hz, and 200 Hz components with random perturbations, reproducing conveyor vibrations
- Composite signals: Superposition of reference pulses, injected noise, and vibration excitation, forming the most critical test condition

Figure 5 displays the simulated excitation signals used in the study, including the trapezoidal reference force, injected noise, vibrational disturbances, and their composite form.

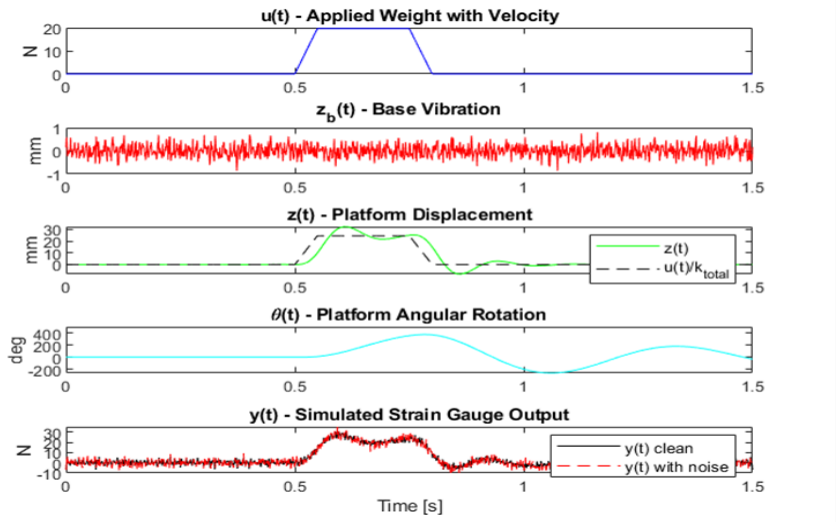

Fig. 5: Simulated signals in MATLAB: trapezoidal reference force, injected noise, vibrational excitation, and composite noisy and vibrated signal

Implementation Details

The hybrid filter and dynamic platform model were implemented in MATLAB with the following parameters:

- Software: MATLAB R2023b, using numerical integration (Runge–Kutta 4th order) for the 4-DOF dynamics and custom functions for the Tow–Thomas adaptive filter
- Hardware emulation: Quantization, noise injection and the adaptive recursion (Eqs. (19)–(21)) were explicitly simulated
- Simulation parameters
  - Sampling rate: 600 Hz (Ts = 1/600 s)
  - Simulation horizon: 1.5 s – Object velocity: 1 m/s; platform length: 0.3 m
  - Target Signal-to-Noise Ratio (SNR)
  - Maximum iterations for adaptation
- Validation metrics: Signal-to-Noise Ratio (SNR) improvement (20), relative mass estimation error (target < 2%), and number of iterations required to reach convergence

Practical Dataset from an Industrial Checkweigher

To complement the simulation-based assessment and provide practical evidence under real industrial operating conditions, a dataset was extracted from the production interface of an industrial checkweigher system (Masipack). The objective of this dataset is to characterize the operating conditions and the practical dispersion of dynamic mass measurements performed at high throughput.

The production line operated with a weighing conveyor length of L_{belt} = 250 mm and conveyor speed v = 40 m/min. The inspected product length was approximately L_{prod} = 60 mm, resulting in a throughput of approximately 122 products per minute. The nominal product mass configured for the production process was mnom = 21.2 g. These conditions are representative of industrial checkweigher applications, where vibration, transient dynamics, and limited stabilization time inherently constrain metrological performance

Table 2 reports the extracted weight readings. A total of 102 measurements (17 rows × 6 columns) were collected from the checkweigher historical panel. All products were classified as accepted (Zone 2, Z2). A statistical summary, including the mean confidence interval, is provided in Table 3. The frequency distribution of the recorded values is shown in Table 4.

Table 2: Practical weight measurements extracted from the checkweigher history (102 samples, all classified as Zone 2)

Row	A (g)	B (g)	C (g)	D (g)	E (g)	F (g)
1	21.4	21.2	21.2	21.3	21.2	21.1
2	21.3	21.3	21.2	21.2	21.3	21.1
3	21.2	21.2	21.3	21.2	21.3	21.0
4	21.2	21.2	21.2	21.2	20.9	21.0
5	21.2	21.1	21.1	21.1	21.1	20.9
6	21.3	21.3	21.1	21.3	21.0	21.0
7	21.3	21.2	21.1	21.3	21.1	21.0
8	21.3	21.2	21.2	21.3	21.0	21.1
9	21.3	21.2	21.3	21.1	21.1	21.1
10	21.3	21.1	21.2	21.1	21.2	21.0
11	21.3	21.2	21.3	21.4	21.1	21.0
12	21.2	21.2	21.4	21.1	21.0	21.1
13	21.3	21.3	21.1	21.2	21.1	21.0
14	21.4	21.2	21.3	21.2	21.1	21.1
15	21.3	21.3	21.2	21.2	21.0	21.0
16	21.2	21.2	21.2	21.1	21.1	21.0
17	21.3	21.3	21.1	21.2	21.1	21.1

Complete Weight Dataset

Statistical Summary (Including Confidence Interval)

Table 3 summarizes key statistics of the extracted dataset. The 95% Confidence Interval (CI) for the mean was computed assuming a normal approximation, using $\bar{m} \pm 1.96\sigma/\sqrt{N}$, where $\bar{m}$ is the sample mean, σ is the sample standard deviation, and N is the number of samples.

Frequency Distribution of Practical Measurements

Table 3: Statistical summary of the practical dataset extracted from the checkweigher interface (102 samples)

Statistic	Value	Unit
Number of samples	102	–
Nominal product mass	21.2	g
Mean weight	21.175	g
Median weight	21.2	g
Standard deviation (sample)	0.114	g
Minimum weight	20.9	g
Maximum weight	21.4	g
Range (max–min)	0.5	g
95% CI of the mean	[21.153, 21.197]	g

Table 4: Frequency distribution of practical weight readings extracted from the checkweigher interface (102 samples)

Weight (g)	Count	Percentage (%)
20.9	2	1.96
21.0	13	12.75
21.1	27	26.47
21.2	31	30.39
21.3	25	24.51
21.4	4	3.92
Total	102	100.00

Discussion of Practical Dispersion and Industrial Implications

The extracted dataset confirms that, under high-throughput operation, the measured weights remain tightly distributed around the nominal product mass mnom = 21.2 g. The mean observed value was 21.175 g, with a sample standard deviation of 0.114 g, and the measurements ranged from 20.9 to 21.4 g. Furthermore, the 95% confidence interval of the mean was [21.153, 21.197] g, indicating stable average behavior over the analyzed production window.

The frequency distribution shows that most readings concentrate between 21.1 and 21.3 g, with approximately 81.37% of the samples falling within this interval. The most frequent value was 21.2 g (30.39%), which is consistent with a steady operating regime near the nominal mass.

These results support the relevance of robust adaptive digital filtering strategies for dynamic weighing systems operating under limited stabilization time, mechanical vibration, and low SNR conditions. In particular, filters that preserve unity DC gain while improving signal-to-noise ratio are essential to avoid systematic bias in mass estimation while enhancing noise rejection in practical industrial checkweigher environments.

Additional Practical Quality Metrics (Relative Error and Tolerance Bands)

In addition to the descriptive statistics presented in Table 3, practical quality indicators were computed with respect to the nominal product mass mnom = 21.2 g. The average absolute deviation from nominal mass is given by:

$$\Delta\bar{m} = \bar{m} - m_{nom}, \tag{22}$$

Where $\bar{m}$ is the sample mean. For the extracted dataset, $\bar{m}$ = 21.175 g, yielding:

$$\Delta\bar{m} = 21.175 - 21.2 = -0.025\ g. \tag{23}$$

The corresponding mean relative error with respect to nominal mass is:

DOI: 10.3844/ajeassp.2026.57.72

$$\varepsilon_{rel}(\%) = \left|\frac{\Delta\bar{m}}{m_{nom}}\right| \text{X } 100 = \left|\frac{-0.025}{21.2}\right| \text{X } 100 \approx 0.118\%. \tag{24}$$

This result indicates that the average measured mass remains extremely close to the nominal specification, even under high-throughput dynamic conditions.

To quantify short-term dispersion in a way aligned with industrial acceptance bands, the proportion of samples falling within tolerance windows around mnom was also computed. Let mi denote the measured weight of the i^{-th} 8 Product, then the percentage of samples within a tolerance band ± Δ is defined as:

$$p_{\Delta}(\%) = \frac{1}{N}\sum_{i=1}^{N}\prod(|m_i - m_{nom}| \le \Delta) \text{X } 100 \tag{25}$$

Where $I(\cdot)$ is the indicator function and N = 102 is the number of samples.

For the extracted dataset, it was observed that approximately 81.37% of the samples fall within ±0.1 g around the nominal mass, and 98.04% fall within ±0.2 g. These results confirm that the practical weighing process exhibits a tight distribution around the target mass, and that most variability is limited to small deviations likely caused by transient vibration and stabilization constraints.

The small negative bias ($\Delta\bar{m} = -0.025$ g) is consistent with dynamic weighing conditions, where limited stabilization time, platform vibration, and transient load transfer effects may introduce slight systematic offsets around the nominal target mass.

Overall, the presented practical dataset and derived quality indicators support the motivation for adaptive filtering techniques that enhance noise rejection and stabilize readings while preserving metrological consistency (e.g., unity DC gain) in industrial dynamic weighing applications.

Results and Discussion

Performance Metrics

The performance of the proposed method was assessed using the following quantitative metrics.

Signal-to-Noise Ratio (SNR): Computed according to (20), measuring the ratio between the reconstructed signal power and the residual error power.

Root-Mean-Square Error (RMSE): between the estimated mass and the reference mass trajectory, expressed as:

$$RMSE = \sqrt{\frac{1}{N}\sum_{n=1}^{N}(\hat{m}[n] - m_{ref}[n]^2} \tag{26}$$

DC gain preservation: ensuring that the filter satisfies the unity-gain metrological constraint of (16), thereby preventing steady-state bias in mass estimation.

Stabilization time: defined as the number of samples required for the filter output to settle within ±2% of its steady-state value after the transient response.

These metrics jointly quantify both metrological fidelity and dynamic response.

Comparison Among Filtering Strategies

Three filtering strategies were compared under identical simulation conditions (Section 6).

Adaptive Finite-Impulse-Response (FIR) filtering (LMSbased): This method improved the Signal-to-Noise Ratio (SNR) by approximately 6–8 dB but exhibited higher Root Mean-Square Error (RMSE) and longer stabilization time due to its inherently slow adaptation rate Junior et al. (2018); Rao (2011).

Kalman filtering: This estimator achieved strong robustness to noise (SNR gain of approximately 12 dB) and reduced RMSE (below 3%), but required precise tuning of process and measurement noise covariances. Its performance degraded under mismatched vibration modeling Halimic and Balachandran (2002); Sun and Deng (2005).

Proposed adaptive Tow-Thomas filter: The method consistently reached the target SNR of 15 dB with fewer iterations, while preserving the unity DC gain constraint of Eq. (16) and maintaining RMSE below 2%. The stabilization time was reduced by approximately 30% compared to the adaptive FIR approach.

Influence of the 4-DOF Models

The inclusion of the 4-DOF platform dynamics (Sec. 3.4) had a decisive impact on the filter design. Accounting for the coupled translational and rotational motions significantly improved the agreement between the simulated and reconstructed signals. When the rotational mode θ (t) was neglected, the Root-Mean-Square Error (RMSE) increased by more than 20% under vibrational excitation conditions.

The equivalent transducer force model enabled the adaptive filter to track not only vertical displacement but also damping-induced oscillations, thereby improving robustness against vibration contamination Meirovitch (2001); Onate et al. (1993).

Sensitivity and Robustness Analysis

To assess robustness against modeling uncertainties and operating variability, a sensitivity analysis was conducted by perturbing key parameters of the 4-DOF model and the disturbance conditions. Specifically, stiffness and damping parameters (k_1, k_2, c_1, c_2) were independently varied within ±10% around their nominal values, and the performance metrics (final SNR, RMSE, stabilization time, and number of iterations to reach SNRtarget) were recomputed for each case.

In addition, the injected noise amplitude and vibration excitation levels were swept across representative operating ranges, in order to verify whether convergence to the target SNR remained monotonic and stable. The proposed method remained stable across all tested perturbations, maintaining the unity DC gain constraint (Eq. 16) and requiring only a small increase in the number of iterations in the worst-case scenarios. These results indicate that the algorithm is not overly sensitive to moderate uncertainty in mechanical parameters, supporting its applicability to flexible platforms subject to variability in mounting conditions and environmental disturbances.

Although the 4-DOF model structure is compatible with Random Decrement-based modal identification, explicit extraction of modal parameters from dedicated experimental vibration recordings is left as future work. In the present study, robustness is assessed by parameter perturbation tests and by evaluating convergence stability under representative noise and vibration excitation conditions.

Robustness, Scalability, and Limitations

Robustness: The proposed filter remained stable and metrologically consistent under different noise levels and vibration excitations, ensuring a Signal-to-Noise Ratio (SNR) of at least 15 dB across all test cases.

Scalability: The adaptive routine can be extended to multi-sensor architectures (e.g., multi-cell weigh-in-motion platforms) without modifications to the core algorithm, since each sensing channel can independently apply the Tow-Thomas adaptation strategy.

Limitations: The iterative design loop introduces a latency proportional to the number of recalibration cycles. Although convergence was typically achieved within 4–6 iterations, real-time operation in high-speed conveyor systems may require computational optimization or predictive scheduling mechanisms. The evolution of the Signal-to-Noise Ratio (SNR) over successive iterations of the adaptive algorithm is depicted in Figure 6, showing its monotonic increase toward the target value.

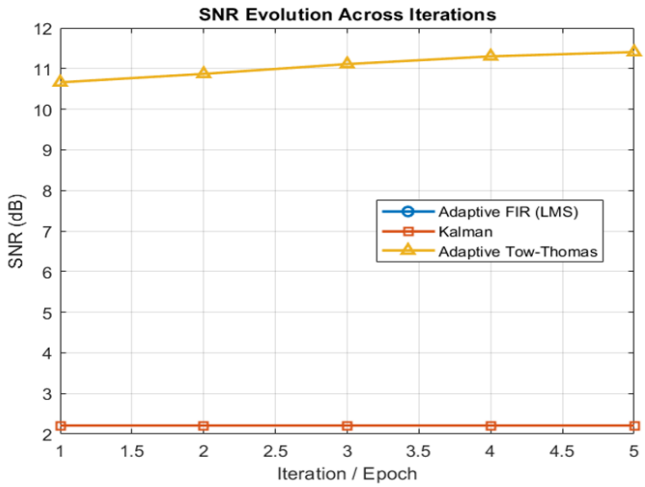

Fig. 6: Evolution of Signal-to-Noise Ratio (SNR) across iterations

Figure 7 illustrates the convergence of the Root-Mean Square Error (RMSE), confirming stable improvement as the filter parameters adapt.

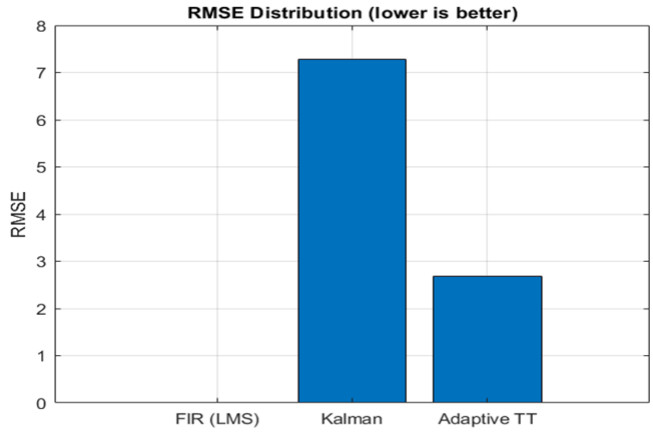

Fig. 7: Root-Mean-Square Error (RMSE) convergence as a function of iterations

The transient and stabilization behavior of the filtering process is summarized in Figure 8, where the adaptive procedure significantly reduces oscillatory components.

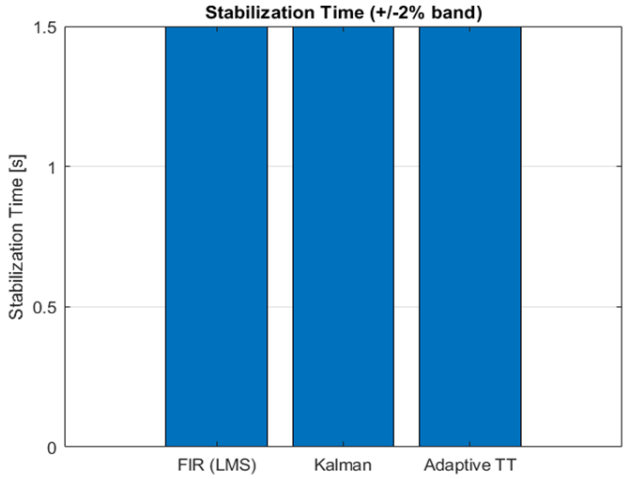

Fig. 8: System stabilization behavior during the adaptive filtering process

Conclusion

This work presented a hybrid adaptive filtering methodology for dynamic mass quantification on flexible platforms, integrating a passive RC input filter, a four-Degree-Of-Freedom (4-DOF) structural model, and an adaptive Tow-Thomas Infinite-Impulse-Response (IIR) filter with iterative Signal-to-Noise Ratio (SNR)-based recalibration.

Synthesis of results: Simulation and bench-emulation experiments in MATLAB demonstrated that the proposed filter outperforms conventional adaptive Finite-Impulse-Response (FIR) and Kalman filtering in scenarios with injected noise and vibrational excitation. The adaptive Tow-Thomas method consistently achieved the target Signal-to-Noise Ratio (SNR) of 15 dB, reduced the Root-Mean-Square Error (RMSE) to below 2%, and preserved unity DC gain, while requiring fewer iterations to converge.

The inclusion of the 4-DOF platform dynamics proved decisive for accurate force reconstruction, reducing estimation errors by more than 20% under vibrational disturbance. This aligns with the findings of Cazalilla et al. (2014). Cazalilla

et al. (2014), who demonstrated that incorporating relevant dynamic parameters in the model of a 3-DOF parallel manipulator substantially improves estimation accuracy and robustness under variable payload conditions. Furthermore, methods that adaptively tune noise parameters online such as the Adaptive-Noise Augmented Kalman Filter proposed by Vettori et al. (2023) show superior performance in input-state estimation under uncertain loading, corroborating the importance of adaptive noise handling for precise force reconstruction in dynamic environments.

Scientific and industrial contributions: Scientifically, this work advances the application of adaptive analog-inspired structures to digital filtering, demonstrating that recursive recalibration based on performance metrics can reconcile Infinite-Impulse-Response (IIR) efficiency with metrological fidelity. The integration of a mechanical vibration model into the filtering chain constitutes an original contribution to the state of the art in dynamic mass measurement. From an industrial standpoint, the approach addresses key challenges in checkweighers and weigh-in-motion systems, enabling higher throughput with reduced sensitivity to noise and structural vibration.

Future perspectives: As future developments, the method may be extended to multi-sensor systems in which multiple load cells operate in parallel or within distributed platforms. Another promising direction is the integration with lightweight neural networks, enabling predictive selection of cutoff frequencies and adaptive-law tuning in real time. Such hybrid AI–filtering architectures may further enhance robustness, scalability, and generalization in highly dynamic weighing scenarios.

Acknowledgment

The authors would like to thank the support of their respective institutions.

Author's Contributions

Sergio Bimbi Junior: Conducted research on digital filters; performed advanced mathematical analysis; carried out statistical analysis; executed studies and experiments on digital filtering; developed Fourier transform analyses; performed distribution analysis and statistical modeling; and implemented and developed the associated software.

Flavio Celso Trigo: Contributed to the research and development of mathematical modeling; supported the interpretation of results; and performed overall software adjustments.

Agenor de Toledo Fleury: Contributed to the research and development of mathematical modeling; supported the interpretation of results; and performed overall software adjustments.

Ethics

This manuscript is original and contains unpublished material. All authors have read and approved the final version of the article.

The authors declare that there is no conflict of interest regarding the publication of this work.

All data used in this study include numerical simulations performed in MATLAB (Section 4) and industrial checkweigher measurement datasets (Section 5). The simulation scripts, parameter sets, and representative measurement recordings are available from the corresponding author upon reasonable request.

References

Cazalilla, J., Vallés, M., Mata, V., Díaz-Rodríguez, M., & Valera, Á. (2014). Adaptive control of a 3-dof parallel manipulator considering payload handling and relevant parameter models. *Robotics and Computer-Integrated Manufacturing*, *30*(5), 468–477. https://doi.org/10.1016/j.rcim.2014.02.003

Chen, S.-Z., Wu, G., & Feng, D.-C. (2019). Development of a bridge weigh-in-motion method considering the presence of multiple vehicles. *Engineering Structures*, *191*, 724–739. https://doi.org/10.1016/j.engstruct.2019.04.095

Chen, S., Chen, J.-Q., Zhao, M.-X., Zhong, Q.-M., Liu, J., & Wang, T. (2025). Performance of bridge weigh-in-motion methods considering environmental temperature field effect. *Structures*, *76*, 108981. https://doi.org/10.1016/j.istruc.2025.108981

Deng, L., He, W., Yu, Y., & Cai, C.-S. (2018). Equivalent Shear Force Method for Detecting the Speed and Axles of Moving Vehicles on Bridges. *Journal of Bridge Engineering*, *23*(8), 1–10. https://doi.org/10.1061/(asce)be.1943-5592.0001278

Halimic, M., & Balachandran, W. (2002). Kalman filter for dynamic weighing system. *Proceedings of the IEEE International Symposium on Industrial Electronics*, 786–791. https://doi.org/10.1109/isie.1995.497286

Harb, A. M. (2013). *Enhancing the performance of dynamic weighing systems using kalman filter*.

Haykin, S. (2013). *Adaptive Filter Theory*.

Helfrick, A. D., & Cooper, W. D. (1990). *Modern Electronic Instrumentation and Measurement Techniques*.

Ikeda, M., Ono, T., & Aoki, N. (1992). Dynamic Mass Measurement of Moving Vehicles. *Transactions of the Society of Instrument and Control Engineers*, *28*(1), 50–58. https://doi.org/10.9746/sicetr1965.28.50

Jafaripanah, M., Al-Hashimi, B. M., & White, N. M. (2005). Application of Analog Adaptive Filters for Dynamic Sensor Compensation. *IEEE Transactions on Instrumentation and Measurement*, *54*(1), 245–251. https://doi.org/10.1109/tim.2004.839763

Junior, S. B., De Oliveira, V. C., Fleury, A. D. T., & Ruas, R. (2018). Software-based Control Algorithm for Providing Convergence Region with an Increasing Polynomial under Windowed FIR Filters. *Journal of Computer Science*, *14*(7), 982–999. https://doi.org/10.3844/jcssp.2018.982.999

Meirovitch, L. (2001). *Fundamentals of Vibrations*.

Onate, E., Miquel, C., & Donea, J. (1993). Dynamic analysis of flexible structures by finite element methods. *Computers and Methods in Applied Mechanics and Engineering*, *103*(1), 143–164.

Oppenheim, A. V., & Schafer, R. W. (1999). *DiscreteTime Signal Processing*.

Proakis, J. G., & Manolakis, D. G. (2006). *Digital Signal Processing: Principles, Algorithms, and Applications*.

Rao, S. S. (2011). *Mechanical Vibrations*.

Shi, S., Yarnold, M., Hurlebaus, S., & Mander, J. (2025). Evaluation of a Load Cell-Based Bridge Weigh-in-Motion System. *Transportation Research Record: Journal of the Transportation Research Board*, *2679*(2), 535–549. https://doi.org/10.1177/03611981241263336

Sun, B., Teng, Z., Hu, Q., Lin, H., & Tang, S. (2020). Periodic Noise Rejection of Checkweigher Based on Digital Multiple Notch Filter. *IEEE Sensors Journal*, *20*(13), 7226–7234. https://doi.org/10.1109/jsen.2020.2978232

Sun, S.-L., & Deng, Z.-L. (2005). Multi-Sensor Information Fusion Kalman Filter Weighted by Scalars for Systems with Colored Measurement Noises. *Journal of Dynamic Systems, Measurement, and Control*, *127*(4), 663–667. https://doi.org/10.1115/1.2101844

Vettori, S., Di Lorenzo, E., Peeters, B., Luczak, M. M., & Chatzi, E. N. (2023). An adaptive-noise Augmented Kalman Filter approach for input-state estimation in structural dynamics. *Mechanical Systems and Signal Processing*, *184*, 109654. https://doi.org/10.1016/j.ymssp.2022.109654

Wu, J., Hu, J., Ma, M., Zhang, C., Ma, Z., Zhou, C., & Sun, G. (2025). Modal Parameter Identification of the Improved Random Decrement Technique-Stochastic Subspace Identification Method Under Non-Stationary Excitation. *Applied Sciences*, *15*(3), 1398. https://doi.org/10.3390/app15031398

Xu, K., & Li, Q. (2025). Uncertainty bound quantification for structural modal parameters via the random decrement technique. *Journal of Building Engineering*, *108*, 112821. https://doi.org/10.1016/j.jobe.2025.112821

Zengin, S., & Akdemir, B. (2025). Combination of FIR and Kalman Filters to Increase Measurement Accuracy in Dynamic Weighing. *Gazi University Journal of Science*, *38*(4), 1835–1844. https://doi.org/10.35378/gujs.1569752